# Antiferrodistortive Reconstruction of the $PbTiO_3$(001) Surface

A. Munkholm,[1,*] S. K. Streiffer,[2] M. V. Ramana Murty,[2,†] J. A. Eastman,[2] Carol Thompson,[2,3] O. Auciello,[2] L. Thompson,[2] J. F. Moore,[2] and G. B. Stephenson[2]

[1]*Chemistry Division, Argonne National Laboratory, Argonne, Illinois 60439*
[2]*Materials Science Division, Argonne National Laboratory, Argonne, Illinois 60439*
[3]*Physics Department, Northern Illinois University, DeKalb, Illinois 60115*

(Received 10 July 2001; published 14 December 2001)

We present *in situ* x-ray scattering measurements of the surface structures of $PbTiO_3$ (001) in equilibrium with PbO vapor. At 875 to 1025 K, a reconstruction having $c(2 \times 2)$ symmetry is present under most conditions, while a $1 \times 6$ reconstruction occurs under PbO-poor conditions. The atomic structure of the $c(2 \times 2)$ phase is found to consist of a single layer of an antiferrodistortive structure with oxygen cages counter-rotated by 10° about the titanium ions.

DOI: 10.1103/PhysRevLett.88.016101 PACS numbers: 68.35.Bs, 61.10.–i, 77.80.Bh, 77.84.Dy

The cubic $ABO_3$ perovskite structure is subject to several competing structural instabilities, which can give rich phase diagrams with structures ranging from polar ferroelectric to nonpolar antiferrodistortive (AFD) [1,2]. The fluctuations near these phase transitions are responsible for the enhanced piezoelectric, dielectric, and ferroelectric properties in perovskites. The presence of a surface can either augment or suppress such structural instabilities and the associated property enhancements. Because of the rapidly increasing use of thin-film perovskites in devices, and their progressive miniaturization, the effects of surfaces on structural phase transitions in perovskites have become an issue of significant practical as well as fundamental interest.

The weakly polar (001) surface of the $ABO_3$ perovskite structure is commonly used for epitaxial growth and has been most extensively studied [3]. The interaction of the surface with bulk instabilities in perovskites has been investigated primarily by surface structure and energy calculations at $T = 0$ K using both shell model [4–6] and *ab initio* density functional theories [7–9]. These studies have found that the outer atomic layers relax and "rumple" normal to the surface, producing a net normal dipole moment even on nonpolar paraelectric bulk phases. For $SrTiO_3$, which forms a bulk AFD phase below 105 K, there has been interest in whether ferroelectric order occurs at the surface. An in-plane surface ferroelectric distortion has been predicted for $SrTiO_3$ using a shell model [5], although more recent *ab initio* calculations indicate that it is very small or absent [7]. Models of ferroelectric $BaTiO_3$ and $PbTiO_3$ [7,8] have found that the ferroelectric order can be either enhanced or suppressed at the surface, depending upon both material and termination. Although the possibility of a cell-doubling AFD surface reconstruction above the $SrTiO_3$ bulk transition has been proposed [4], in all but one of these calculations [5] the bulk $1 \times 1$ in-plane unit cell has been imposed on the surface, and reconstructions have not been explicitly modeled. Until now, experimental studies of perovskite surfaces have concentrated on $SrTiO_3$ [3]. Relaxation and rumpling of unreconstructed surfaces have been measured, although no in-plane ferroelectric order is found [10]. A variety of reconstruction symmetries have been observed on vacuum-annealed surfaces [3,11] and in oxygen environments [12]. These have generally been attributed to point defect ordering [12], although determination of the structure of these reconstructions remains an active area of research [11]. One issue is a lack of definition of the surface stoichiometry produced by the various annealing procedures [3].

In this Letter, we report an experimental study of the (001) surface of $PbTiO_3$. This system is the prototype of a large class of Pb-based perovskites [1]. Since PbO is relatively volatile, we can control its partial pressure ($P_{PbO}$) in the vapor phase and observe the equilibrium surface structure of $PbTiO_3$ under defined cation stoichiometry. In our experiments, grazing incidence x-ray scattering is used to observe the surface structure *in situ* after growth in an organometallic vapor phase epitaxy (OMVPE) system. A $c(2 \times 2)$ reconstruction is present under most conditions, while a $1 \times 6$ reconstruction occurs under PbO-poor conditions. The $c(2 \times 2)$ reconstruction consists of a single layer of an AFD structure with $TiO_4$ cages alternately counter-rotated about [001], as in the low-temperature phase of $SrTiO_3$ [1]. This provides direct evidence for the effect of surface relaxation on the balance of interatomic forces responsible for the AFD instability, and suggests that calculations with unit cells larger than $1 \times 1$ would be useful.

The $PbTiO_3$ samples were epitaxial films grown on $SrTiO_3$ (001) substrates using a facility for *in situ* x-ray measurements during and after OMVPE growth [13] on BESSRC beam line 12-ID-D at the Advanced Photon Source. Tetraethyl lead (TEL), titanium isopropoxide (TIP), and $O_2$ were used as the precursors for OMVPE growth, with N2 carrier gas. The films were deposited at 950–1000 K at a total pressure of 10 Torr ($P_{O_2} = 2.5$ Torr). The samples were maintained at high temperature and flowing TEL for *in situ* x-ray characterization after growth, which minimized opportunities

  

for introduction of impurities. Because $O_2$ is always present in excess, the value of $P_{PbO}$ in equilibrium with the surface at high temperature is expected to be equal to the partial pressure of TEL in the input flow. Films 75 to 800 Å thick were studied, and the surface structure was found to be independent of film thickness. All films replicated the high crystalline quality of the substrates (0.01° typical mosaic). Films thinner than 400 Å remained lattice matched with the $SrTiO_3$, while the ~1% compressive epitaxial strain was mostly relaxed in thicker films. Scattering measurements were carried out using 24 keV x rays selected by a Si(111) monochromator. Incidence and exit angles were kept at the critical angle (0.13°).

By varying $T$ and $P_{PbO}$ while observing the in-plane scattering pattern, we mapped the equilibrium phase diagram of the $PbTiO_3$ (001) surface. Over the region of conditions investigated, two surface phases were observed having $c(2 \times 2)$ and $1 \times 6$ symmetries. Figure 1 shows the resulting surface phase diagram and characteristic

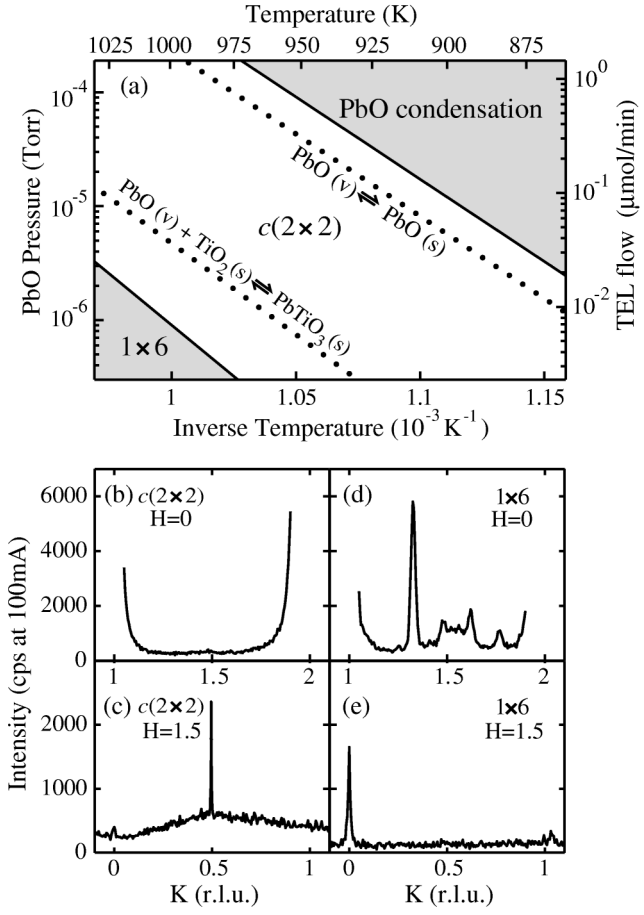


FIG. 1. (a) Equilibrium phase diagram of the $PbTiO_3$ (001) surface showing the region investigated. Solid lines separate phase fields corresponding to PbO condensation, $c(2 \times 2)$, and $1 \times 6$ reconstructions. Dotted lines are literature values [14] for the PbO condensation and $PbTiO_3$ decomposition boundaries. (b)–(e) Characteristic in-plane scans ($L \approx 0$) of the $c(2 \times 2)$ and $1 \times 6$ reconstructions at 1005 K. For (b) and (c), $P_{PbO} = 2.4 \times 10^{-6}$ Torr; for (d) and (e), $P_{PbO} = 3 \times 10^{-7}$ Torr.

in-plane diffraction patterns of the two reconstructions. The surface structure could be reversibly and reproducibly switched between these two reconstructions by changing $T$ or $P_{PbO}$ to cross the phase boundary shown [lower solid line in (a)]. At high input flows of TEL and lower temperatures, diffraction peaks from the condensation of polycrystalline PbO began to appear. The observed TEL input pressure at which PbO condensed (upper solid line) is approximately a factor of 2 larger than the literature value for the equilibrium PbO condensation pressure [14] (upper dotted line), validating the equality of $P_{TEL}$ in the input flow and $P_{PbO}$ at the sample surface, within this factor. Also shown in Fig. 1(a) (lower dotted line) is the boundary below which bulk $PbTiO_3$ is metastable with respect to $TiO_2$ [14]. Even with zero TEL flow, the only evidence of $PbTiO_3$ decomposition we observed at these temperatures was the formation of the $1 \times 6$ reconstruction, indicating that bulk decomposition is sluggish. Within the range of conditions investigated, the equilibrium surface phase is the $c(2 \times 2)$ structure over the complete equilibrium phase field of bulk $PbTiO_3$, *i.e.,* between the dotted lines in Fig. 1(a).

We always observed the $1 \times 6$ reconstruction to have relatively broad diffraction peaks, indicating that it was not well ordered, and we have not attempted to model its atomic structure. However, the sharp diffraction peaks observed for the $c(2 \times 2)$ reconstruction indicate that it is very well ordered, with typical rocking widths (e.g., 0.08° for the $\frac{3}{2}\frac{1}{2}0$) corresponding to a domain size of ≥1800 Å. To determine the structure of this reconstruction, we measured the integrated intensities of 14 independent in-plane reflections with the sample at 905 K and $P_{PbO} = 4 \times 10^{-6}$ Torr. Checks of symmetry-related peaks showed that the diffraction pattern has fourfold and mirror symmetries. We found that the $c(2 \times 2)$ intensities did not vary significantly with changes in $P_{PbO}$ within the phase field shown in Fig. 1(a), did not vary with changes in $P_{O_2}$ within the range 0.5–7.5 Torr, and varied only weakly over the temperature range 875–1025 K consistent with the Debye-Waller factor, suggesting that it is a stoichiometric structure without large concentrations of defects. The $c(2 \times 2)$ reconstruction remained even at room temperature after cooling under appropriate conditions. In order to compare the 905 K data set to models in absolute units, we extracted structure factors $|F_{exp}|$ from the measured integrated intensities by applying polarization, geometry, and Lorentz corrections [15]. These are shown in Fig. 2. Since bulk $PbTiO_3$ Bragg peaks occur at positions with $h + k$ even, the $c(2 \times 2)$ reconstruction peaks are those with $h + k$ odd. Zero intensity above background was found at all reconstruction positions having either $h = 0$ or $k = 0$.

The systematic absences at $h = 0$ and $k = 0$ and the small unit cell size greatly restrict the potential structural models. To produce these absences, the symmetry of the

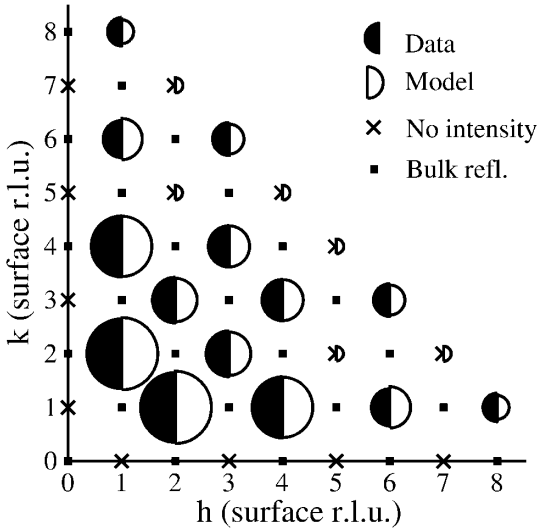


FIG. 2. Structure factors for the $c(2 \times 2)$ reconstruction, plotted vs surface Miller indices $h$ and $k$ for the primitive $(\sqrt{2} \times \sqrt{2})R45°$ unit cell (related to bulk indices $H, K$ by $h = H + K$; $k = K - H$). Areas of filled and open half circles are proportional to observed and calculated structure factors.

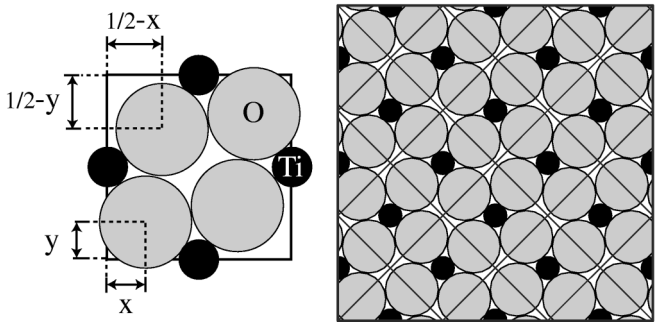


FIG. 3. Schematic of the $TiO_2$ layer in the antiferrodistortive model for the $c(2 \times 2)$ $PbTiO_3$ (001) reconstruction, showing counter-rotated O cages. The square grid at 45° shows the underlying bulk $PbTiO_3$ unit cells. Expanded view: the $(\sqrt{2} \times \sqrt{2})R45°$ primitive surface unit cell.

structure must be at least that of plane group $p2gg$, with glide planes perpendicular to both axes [16]. This requires identical motifs in at least four in-plane positions per primitive unit cell, at positions $(+x, +y)$, $(-x, -y)$, $(\frac{1}{2} + x, \frac{1}{2} - y)$, and $(\frac{1}{2} - x, \frac{1}{2} + y)$ in fractional coordinates. Out-of-plane studies of the reconstruction peaks showed that their integrated intensities decreased by less than 50% as $L$ increased to 2.5 $Å^{-1}$, indicating that the reconstruction consists of a single layer of atoms. We first considered structures with nominally neutral combinations of cations and anions in the layer, which are considered to be energetically most favorable [3]. Structures based on a PbO layer are ruled out because there is not enough space in the $(\sqrt{2} \times \sqrt{2})R45°$ surface unit cell (a 5.6 Å square) to accommodate four $Pb^{2+}$ and four $O^{2-}$ ions (ionic radii 1.49 and 1.40 Å [17], respectively). The only such structure that fits within the unit cell is a $TiO_2$ layer with four $O^{2-}$ ions at the $p2gg$ general positions, and two $Ti^{4+}$ ions at the $1 \times 1$ positions $(0, \frac{1}{2})$ and $(\frac{1}{2}, 0)$. Figure 3 shows a diagram of this structure, which gives the best fit to the data of all models tested. It can be described as a $BO_2$ perovskite layer with O cages rotated about the B ions in an alternating fashion. This cage rotation forms the AFD structure associated with a soft $R_{25}$ phonon mode occurring in many bulk $ABO_3$ perovskites [2].

Following standard procedures [18], we refined the structure of the AFD layer model by fitting using four parameters: $\bar{x} \equiv (x + y)/2$, $\Delta x \equiv (x - y)/2$, $u$, and $C$. Here $u$ is the rms vibrational amplitude of the oxygen ions, and $C$ is a scale factor in $|F_{\text{calc}}|$ to account for uncertainty in the absolute normalization of $|F_{\text{exp}}|$. Since this four-parameter fit yielded $\Delta x = 0.011 \pm 0.026$, consistent with a symmetric displacement $(x = y)$, we also performed a three-parameter fit with $\Delta x$ fixed at zero. The latter was statistically preferable, with a crystallographic residual $R = 0.012$ indicating a very good fit, yielding $\bar{x} = 0.206 \pm 0.004$, $u = 0.19 \pm 0.03$ Å, and $C = 0.61 \pm 0.08$. The structure factors from this fit are shown in Fig. 2. The value of $\bar{x}$ corresponds to a rotation of the oxygen cages by $10° \pm 1°$. The value of $u$ compares quite reasonably with 0.15 Å for bulk $PbTiO_3$ at 905 K [19]. The value of $C$ is consistent with unity, within the uncertainty in the determination of the absolute scale. This agreement uniquely supports the AFD layer model for the $c(2 \times 2)$ reconstruction in which only individual oxygen ions are located at each $p2gg$ general position, since all alternative models have contributions from heavier ions which produce much larger structure factors than observed.

Since the reconstruction peaks are insensitive to the nature of the ions occupying the $1 \times 1$ positions, we also considered the possibility that they could be $Pb^{4+}$ rather than $Ti^{4+}$ ions. The observed cage rotation increases the space between the oxygens by 5%, which could be interpreted as partial accommodation of the 30% larger $Pb^{4+}$ ions. To test this hypothesis, we made *in situ* measurements at 1005 K of the intensities of the $11L$, $20L$, and $21L$ crystal truncation rods as a function of $L$, which are sensitive to the type of ions in the $1 \times 1$ positions [20]. These results are more consistent with $Ti^{4+}$ than with $Pb^{4+}$ ions. In addition, we made *ex situ* room-temperature Mg $K_\alpha$ x-ray photoemission spectroscopy measurements of the Pb $4f$ peaks, which show no evidence for multiple valence states of Pb in the top ~20 Å of the sample. Thus, we believe the B sites are occupied by $Ti^{4+}$ ions in the reconstructed layer.

Although the x-ray data show that the $c(2 \times 2)$ reconstruction consists of a single $TiO_2$ layer with rotated oxygen cages, neither the reconstruction peaks nor the crystal truncation rods are sensitive to whether this layer

terminates the $PbTiO_3$ surface, or instead is covered by an unreconstructed PbO layer. Since theory predicts that only the PbO-terminated surface is stable [8], and the observed phase diagram shows that the $c(2 \times 2)$ reconstruction is PbO-rich compared with the $1 \times 6$ phase, the presence of a PbO termination layer is plausible. We found that the $1 \times 6$ phase could be formed from the $c(2 \times 2)$ phase at lower temperatures and zero TEL flow by introducing TIP equivalent to $\sim$1 monolayer of $TiO_2$, suggesting that either the $c(2 \times 2)$ phase is PbO terminated or the $1 \times 6$ phase is terminated by two consecutive $TiO_2$ layers.

Shell model calculations have predicted that an AFD surface reconstruction may occur in $SrTiO_3$ at temperatures above the bulk AFD transition, owing to stabilization by the surface relaxation [4]. Although bulk $PbTiO_3$ becomes ferroelectric rather than forming an AFD phase, a weak instability with respect to the AFD phase has been predicted in *ab initio* models [2,21]. In general, the AFD instability is expected to depend strongly on the relative sizes of the A and the B ions [2], hydrostatic pressure [22], and strain fields around defects [23], because of a competition between long-range Coulombic and short-range interatomic forces. A change in the balance of these forces at the surface is presumably responsible for the observed AFD structure of the $PbTiO_3$ surface. Since the ferroelectric and AFD instabilities typically result from opposite changes in this balance [2,22], the AFD surface reconstruction of $PbTiO_3$ may be related to the "dead layer" often postulated to explain the observed decrease in ferroelectric character in thin films.

The epitaxial constraint of a $SrTiO_3$ substrate is expected to increase the ferroelectric transition temperature of a $PbTiO_3$ film above the bulk value (765 K) [24]. We have found that the $PbTiO_3$ films used in this study can indeed be either paraelectric or ferroelectric (with polarization normal to the surface) in the temperature range 875–1025 K, depending on epitaxial strain and film thickness [25]. However, the same $c(2 \times 2)$ surface structure occurs on both ferroelectric or paraelectric films. This is consistent with theoretical results showing that the surface relaxation energies are generally much larger than the energy changes associated with the bulk ferroelectric instability [8]. In addition, since the $c(2 \times 2)$ structure occurs on both coherent and relaxed films, epitaxial strain is not responsible for its formation.

Since the conditions under which the $c(2 \times 2)$ reconstruction occurs are typical of those used in OMVPE and other deposition processes for Pb-based perovskite films, the AFD structure found in this study may be directly relevant to many systems. The $1 \times 6$ reconstruction occurs under conditions at which $TiO_2$ is the equilibrium solid phase, and is thus likely to be a nonequilibrium structure representing the first step in decomposition of $PbTiO_3$. Some of the many surface reconstructions observed for $SrTiO_3$ may also fall into this class.

This work is supported by the U.S. Department of Energy, BES-DMS, under Contract No. W-31-109-ENG-38, and the State of Illinois under HECA.

*Current address: Lumileds Lighting, 370 W. Trimble Road, San Jose, CA 95131.
Electronic mail: anneli.munkholm@lumileds.com
†Current address: E2O Communications Corp., 26679 W. Agoura Road, Calabasas, CA 91302.

[1] M. E. Lines and A. M. Glass, *Principles and Applications of Ferroelectrics and Related Materials* (Clarendon, Oxford, 1977), p. 260.
[2] W. Zhong and D. Vanderbilt, Phys. Rev. Lett. **74**, 2587 (1995).
[3] C. Noguera, J. Phys. Condens. Matter **12**, R367 (2000).
[4] J. Prade *et al.,* J. Phys. Condens. Matter. **5**, 1 (1993).
[5] V. Ravikumar, D. Wolf, and V. P. Dravid, Phys. Rev. Lett. **74**, 960 (1995).
[6] E. Heifets, E. A. Kotomin, and J. Maier, Surf. Sci. **462**, 19 (2000).
[7] J. Padilla and D. Vanderbilt, Phys. Rev. B **56**, 1625 (1997); Surf. Sci. **418**, 64 (1998).
[8] B. Meyer, J. Padilla, and D. Vanderbilt, Faraday Discuss. **114**, 395 (1999).
[9] R. E. Cohen, Ferroelectrics **194**, 323 (1997); Z.-Q. Li *et al.,* Phys. Rev. B **58**, 8075 (1998); C. Cheng, K. Kunc, and M. H. Lee, Phys. Rev. B **62**, 10 409 (2000).
[10] G. Charlton *et al.,* Surf. Sci. **457**, L376 (2000).
[11] T. Kubo and H. Nozoye, Phys. Rev. Lett. **86**, 1801 (2001).
[12] Q. D. Jiang and J. Zegenhagen, Surf. Sci. **425**, 343 (1999).
[13] G. B. Stephenson *et al.,* Appl. Phys. Lett. **74**, 3326 (1999).
[14] I. Barin, *Thermochemical Data of Pure Substances* (VCH, New York, 1995), 3rd ed.
[15] E. Vlieg, J. Appl. Crystallogr. **30**, 532 (1997).
[16] H. Lipson and W. Cochran, *The Determination of Crystal Structures* (Bell, London, 1953), p. 29.
[17] R. D. Shannon and C. T. Prewitt, Acta Crystallogr. Sect. B **25**, 925 (1969).
[18] *International Tables for X-ray Crystallography,* edited by J. S. Kaspar and K. Lonsdale (Kynoch, Birmingham, 1972), Vol. II, pp. 326–328.
[19] A. M. Glazer and S. A. Mabud, Acta Crystallogr. Sect. B **34**, 1065 (1978).
[20] R. Feidenhans'l, Surf. Sci. Rep. **10**, 105 (1989).
[21] P. Ghosez *et al.,* Phys. Rev. B **60**, 836 (1999).
[22] G. A. Samara, T. Sakudo, and K. Yoshimitsu, Phys. Rev. Lett. **35**, 1767 (1975).
[23] R. Wang, Y. Zhu, and S. M. Shapiro, Phys. Rev. Lett. **80**, 2370 (1998).
[24] N. A. Pertsev, A. G. Zembilgotov, and A. K. Tagantsev, Phys. Rev. Lett. **80**, 1988 (1998).
[25] S. K. Streiffer *et al.* (unpublished).